

Urban Expansion and the Global Network of Protected Areas

David Potere
Office of Population Research
Princeton University
dpotere@princeton.edu

Annemarie Schneider
Center for Sustainability and the Global Environment
University of Wisconsin-Madison
aschneider4@wisc.edu

1. INTRODUCTION

The goal of this research is to explore the global-scale vulnerability of protected areas¹ to urban settlement, both now, and over the next several decades. Prior to 2000, if one asked the simple questions, “How much of the Earth is urban, how much is designated for conservation, and what is their spatial relationship?” data quality, consistency, and availability would not have been up to the task. Those constraints have changed. Over the past five years, international research groups from both government and academia have produced seven global-scale urban maps. The conservation community has undertaken a similar surge in mapping efforts, constructing detailed maps of biodiversity hotspots and eco-regions (Myers et al. 2000; Olson et al. 2001), and significantly improving the spatial and temporal properties of the World Database of Protected Areas (WDPA; Chape et al. 2005).

This new suite of maps, and associated advances in satellite remote sensing and geographic information systems (GIS), could not have arrived at a more fortuitous time for conservation. Today, more than 2.07 billion people live within the biodiversity hotspots of Meyers et al. (2000).² World population is expected to grow by nearly two billion through 2030, and almost all of that growth will likely occur within the cities of the developing world (UN 2005; Montgomery 2008). This rapid global urbanization implies an equally-rapid global urban expansion³ (Angel et al. 2005). Certainly these

¹ A protected area as defined by the Convention on Biological Diversity is “a geographically defined area which is designated or regulated and managed to achieve specific conservation objectives.”

² Based on our analysis of Conservation International’s 34 biodiversity hotspots (<http://www.biodiversityhotspots.org/>), and the 2006 release of the LandScan population map (<http://www.ornl.gov/sci/landscan/>).

³ Urbanization refers to increases in the fraction of a population living in urban areas, and urban expansion refers to physical growth in the areal extent of cities.

demographic forces will impact the world's protected areas, yet today the magnitude and spatial distribution of these potential impacts remains poorly constrained.

We begin this section with a brief review of available datasets and the relevant literature (**Section 1**). Next, we select the most accurate global urban map (**Section 2**) and overlay this map on the WDPA in order to characterize the urban proximity of protected areas both globally and regionally (**Section 3**). We then use a recent set of country-level demographic time series derived from the Intergovernmental Panel on Climate Change scenarios (IPCC-SRES; Grubler et al. 2007) together with a simple model for urban growth to estimate the outer envelope of future urban expansion through 2100 at 500 m resolution (**Section 4**). Finally, we briefly discuss some of the limitations of this work and outline future research directions (**Section 5**).

1.1 Conservation datasets

The 2007 World Database of Protected Areas (WDPA) is a global inventory of more than 108,000 conservation areas produced by the World Conservation Monitoring Center (WCMC), in partnership with the United Nations Environment Programme (UNEP; Chape et al. 2005). In the most recent 2007 version, 77.5% percent of the WDPA inventory is classified using the International Union for Conservation Nature (IUCN) categories (Table 1). Within the seven IUCN classes, we construct two groups: (1) *IUCN-high*: areas of strict protection and low levels of intrusion by the built environment (classes I-IV), and (2) *IUCN-low*: areas of less-stringent protection and a significant presence of built environment (classes V-VI). The remaining WDPA sites have not yet been classified according to the IUCN system, and can be grouped into three

classes (Table 2): internationally-designated, nationally-designated, and un-designated areas. The internationally-designated areas are defined in three separate treaties: World Heritage Areas, Ramsar wetlands, and UNESCO Man and the Biosphere Reserves (MAB).

[Table 1, about here]

Although the WDPA has made significant strides in improving the spatial qualities of the inventory, there remain significant overlaps between sites. For this study, we converted all of the land-based protected areas into a 30" arc-second global raster, and resolved conflicts by prioritizing IUCN-classes first, followed by international treaties, and lastly, national designations. We did not consider un-designated candidate areas. The total coverage of conflict-resolved protected areas is 16.8 million sq. km.⁴ From the continental bar plots of in Figure 1, it is clear that Latin America and the Caribbean have the most land within the WDPA, followed closely by Asia and Oceania, and North America.⁵ In terms of the most closely guarded *IUCN-high* land (shaded red), North America has by far the largest holdings, followed by Africa.

[Figure 1, about here]

⁴ Our total differs from Chape et al.'s (2005) estimate of 18.4 million sq. km because we account for overlapping designations, and we use the updated 2007 WDPA. There may also be some small differences due to our gridding of the WDPA polygons, but this difference is less than 1000 sq. km.

⁵ For coding continental regions, we use the UN Statistics Division's major areas (UN 2008).

1.2 Global urban maps

For conservation land, the WDPA is the only global data source. The story is far more complex for urban areas. There are seven global-scale maps that can be used to represent urban areas circa-2000 and two more that portray attributes closely associated with urban land (Table 2). These maps draw on a complex and often overlapping mix of census results, satellite remote sensing data, and GIS data layers (Potere and Schneider, 2007). Because of the lack of a widely-recognized definition of urban land and the heterogeneity of the urban signature, these seven maps exhibit an order of magnitude variance in the total extent of urban area (Figure 2). For perspective, the difference between the largest and smallest extent in Figure 2 is roughly equal to the land area of India. This variation persists across world regions and a wide range of spatial resolutions (Potere and Schneider, 2007), prompting us to conduct a map assessment in Section 2, by using a global sample of 120 city-scale maps.

Part of the heterogeneity of these urban maps extends to map projection, resolution, and classification type (Table 2). In order to compare and assess the maps we converted each to a geographic projection, WGS-84 datum, and a 30'' arc-second raster (~0.86 sq. km cells, at the equator).⁶ We checked the modified maps against their native counterparts for consistency at each stage in the conversion process, and differences were negligible. In order to make international comparisons between maps, we relied on the 30'' arc-second boundary file from the LandScan 2006 population dataset (Table 2) as a base, and expanded the land-water boundary in order to accommodate all of the urban

⁶ We also made the same modifications to Global Landcover 2000 that were first reported in Potere and Schneider (2007); we included updated urban maps from the Global Landcover 2000 team.

land in each map.⁷ Carefully dealing with land-water boundary is important because of the large number of coastal cities.

[Table 2, about here]

[Figure 2, about here]

1.3 Literature review

Global-scale research has only recently begun to address the intersection of biodiversity, conservation, and urban expansion. The improved WDPA dataset, together with new global maps of species prevalence have prompted a series of global-scale studies aimed at assessing the adequacy of the world's protected areas for conserving biodiversity (Brooks et al. 2004; Rodrigues et al. 2004; Chape et al. 2005). Recent studies have also examined links between species diversity and human settlement at regional to global scales (Davies et al. 2006). Yet thus far, the few studies that have explored urban expansion and protected areas were conducted prior to the advent of global urban maps (Morris and Kingston 2002), or were regional in scope (Ricketts and Imhoff 2003). This research is the first moderate-resolution look at the impact of global urban expansion upon the world's protected areas.

At sub-global scales, there is a much richer literature exploring the many ways that urban areas alter their surrounding ecosystems (Grimm et al. 2008), including: species diversity (Pauchard et al. 2006; Burgess et al. 2007), microclimate (Unger 2001),

⁷ The names of the 223 countries recognized by LandScan (US Census) were cross-walked to the International Organization for Standardization (ISO) codes, and then linked to the major area and world region scheme of the UN Statistics Division (UN 2008).

phenology and net primary production of urban-proximate vegetation (Zhang et al. 2004), and global climate and biogeochemical systems (Calbo et al. 1998; Peters-Lidard et al. 2004). There is little doubt that the influence of urban areas extends beyond their immediate neighborhoods, altering ecosystems at considerable distances (Rees 1992; Folke et al. 1997; Alberti 2005). For this reason, we are concerned not only with urban encroachment on conservation lands, but also with the proximity of conservation lands to large urban areas. Such proximity may reduce the effectiveness of existing protected areas, and certainly increases the cost of conservation management (Bruner et al. 2004).

2. SELECTING A GLOBAL URBAN MAP

The seven global urban maps are evaluated using a two-stage accuracy assessment, where a sample of medium-resolution maps with known accuracy is used to assess the coarse resolution maps. For this medium-resolution assessment sample, we turn to the Angel et al. (2005) global urban expansion project (Figure 3). The Angel et al. cities are a global stratified random sample of the roughly 4,000 cities with populations greater than 100,000, where the stratification was conducted with respect to city population size, GDP, and geographic region.⁸ Angel et al. mapped these 120 cities using medium resolution (28.5 meter) imagery, which is an order of magnitude finer than the highest resolution images used to construct the global urban maps. Because of this advantage in spatial resolution, we can place greater confidence in the ability of expert judgment and unsupervised classifiers to accurately portray the built environment in these

⁸ Data from the Dynamics of Global Urban Expansion project can be found at the Center for Land Use Education and Research (CLEAR) website, <http://clear.uconn.edu>.

maps; Angel et al. report an 89.2% overall map accuracy. As a final check on the overall quality of these maps, we geo-located the cities in the Google Earth archive.

[Figure 3, about here]

The Angel et al. cities are used in three separate assessment analyses. We begin by searching for omitted cities (Section 2.1), next we compare each of the seven global-scale maps with local-scale city maps to assess their ability to correctly map urban extent (Section 2.2), and finally we use the same local-scale maps to examine the ability of the coarse resolution global maps to accurately portray urban form (Section 2.3).

2.1 Assessing urban omission errors

We begin our assessment by searching for cities from the Angel et al. (2005) sample that are omitted by the global coarse-resolution maps. An important quality of these global urban maps is their ability to replicate the information content of leading city gazetteers, which list the position and population of major cities worldwide. Table 3 presents a summary of the omissions, where we consider any city with less than five sq. km of urban extent in a given map as omitted by that map⁹ (from here forward, we rely on the map abbreviations introduced in Table 2). There are seven Asian cities of more than 1 million people that were omitted in at least one of the global urban maps. Overall, GLC00, and VMAP0 have the highest omission rates from our sample (mean of 10%), MOD500 and IMPSA have no omissions, and the rest are intermediate (mean of 2%).

⁹ We selected a 5 sq. km threshold after establishing that the overall pattern of omissions is robust with respect to omission thresholds in the 1-10 sq. km range.

Only one developed-country city was omitted; Fukuoka, Japan, with a population of 1.3 million people was omitted by GLC00. Overall, MOD500 and IMPSA emerge as the maps which are least likely to omit cities.

[Table 3, about here]

2.2 Assessing the overall extent of cities

A natural extension of this search for omission errors is to plot the areal extent of each assessment city against the extent mapped for the same area by each of the global urban maps. The log-log scatter plots of Figure 4 compare the assessment city size (x-axis) with the size mapped by each of the 120 global urban maps (y-axis), where the blue diagonal marks perfect inter-map agreement. It is clear that VMAP0 underestimates urban extent (upper-left), GRUMP overestimates urban extent (lower-middle), and MOD500 does the best job of reproducing the areal extents of the assessment cities (middle-right). This visual observation is confirmed by the Pearson correlation coefficients: MOD500 is highest at 0.95; HYDE3, IMPSA, and MOD1K are between 0.83 - 0.87; and the rest range from 0.60 – 0.77.

[Figure 4, about here]

2.3 Assessing the spatial pattern of cities

It is possible for a map to correctly estimate the areal extent of a city, and describe a city shape that completely fails to conform to that of the assessment map. Because our

assessment is conducted at 30'' arc-second resolution, serious distortions in the shape of a city could lead to errors in our comparison with the WDPA. In order to test for overall map agreement, we begin by constructing a contingency table for each city-map combination, where we overlay each map-pair and record the extent of agreement and disagreement (Table 4). From these contingency tables, it is possible to estimate several statistics that measure overall map agreement, adjusting for differences in the overall extent of the maps and differences due to random chance. Cohen's kappa is a widely-used member of this group of statistics (Cohen 1960; Congalton and Green 1999; Table 4). Each map's distribution of 120 Cohen's kappa statistics is described in the box-plots of Figure 5, where values of 1.0 indicate perfect inter-map agreement.¹⁰ The IMPSA and MOD500 maps are in significantly better agreement with the Landsat assessment maps, and this finding is robust across two other widely used map agreement statistics.¹¹

[Table 4, about here]

[Figure 5, about here]

Based on these measures of map accuracy, the best overall choice is MOD500, the new 500 m resolution urban map derived from MODIS satellite imagery. IMPSA was another possible candidate, performing as well on the urban omission (Section 2.1) and overall map accuracy test (Section 2.3), but we select MOD500 based on superior

¹⁰ The asterisks adjacent to HYDE3 and IMPSA indicate that we used thresholded versions of those maps, where majority-urban pixels ($\geq 50\%$ urban) were labeled as urban and all others as non-urban.

¹¹ Normalized mutual information (Forbes 1995), and true skill statistic (Allouche et al. 2006).

performance in Section 3.2 and MOD500's higher spatial resolution (500 m versus 1 km). MOD500 is the global urban map used to estimate urban proximity in Section 3 and to model urban growth in Section 4. There are several limitations to this map accuracy assessment, including: the adequacy of the validation sample, potential geo-location errors, and temporal mismatches between the global urban maps and the assessment maps. With regard to the former, our sample of 120 city maps was drawn from cities with more than 100,000 persons, which excludes 26% of the global urban population (Angel et al. 2005; UN 2005). Work is ongoing to address some of these shortcomings.

3. URBAN-PROXIMITY OF PROTECTED AREAS

Figures 6a and 6b depict both the MOD500 urban map and the WDPA at a global scale. The yellow to red color ramp indicates the urban fraction of each pixel and dark blue areas are urban-free. In Figure 6b, the red patches are IUCN-classified protected areas and the blue patches are non-IUCN.¹² By overlaying these two maps, we can identify regions of intersection (Section 3.1), and assess urban proximity (Section 3.2).

[Figure 6, about here]

3.1 Urban inholdings and incursions

We begin with a look at the most urban-proximate protected areas—those areas mapped as both 'urban' in MOD500 and 'protected' in the WDPA. An overlapping pixel can be explained in one of four ways: (1) it is an erroneous pixel in the urban map and is

¹² The methodology used to create Figure 6 relies on a hexagonal system of discrete global grids (Sahr et al. 2003), and was first described in Potere and Schneider (2007).

not actually urban (an urban commission error), (2) it is an erroneous pixel in the WDPA and is not actually protected (a protected commission error), (3) it is an urban inholding, an area of built environment that existed prior to the establishment of the conservation area and a common occurrence in IUCN category V or VI lands, or (4) it is urban incursion, an area of relatively new urban land that has extended into the protected area after its establishment. Only high resolution imagery or a site visit can resolve the status of each overlap. Given the large area of overlaps, such an undertaking is beyond the scope of this research. Until a significant sample of these overlaps can be assessed, our findings should be regarded as a preliminary indication of the overall pattern of inholdings and incursions.

The box-plots of Figure 7 describe the distribution of overlaps between the classes of protected areas (described in Table 1) and the seven global urban maps (described in Table 2). Among the four categories of WDPA land, *IUCN-low* is by far the one most often overlapped with an urban map. This is not surprising when one considers that many IUCN class V lands contain the human built environment by design (Table 1). Across all four classes, the overlap area is small relative to the overall extent of the entire WDPA; globally, overlaps represent just 0.12% of the 16.8 million sq. km of protected land. However, in absolute terms, the 20,200 sq. km. of overlap is considerable. For scale, Yosemite National Park in the US is roughly 3,000 sq. km, and the maximum value for the *IUCN-low* class is nearly 15,000 sq. km—five times the size of Yosemite. Based on the width of the inter-quartile ranges in Figure 7, it is clear that the degree of overlap between urban and conservation areas is highly sensitive to map selection. This sensitivity was the motivation for the map assessment in Section 2.

[Figure 7, about here]

The red dots in Figure 7 represent the overlap reported by MOD500, the urban map which we use from this point forward. We can decompose the overall area of MOD500 overlap according to world region (Figure 8, Table 5). From Figure 8, it is clear that Europe is the region with the largest amount of urban inholdings or incursions on conservation areas, in both absolute and relative terms (nearly 10,000 sq. km, or 0.42% of all European protected areas). This is surprising considering that Europe has the smallest overall extent of protected areas (Figure 1). Asia and Oceania, North America, and Latin America and the Caribbean are all roughly equal at just under 4,000 sq. km of urban inholdings and incursions. Africa has by far the least amount of overlap, both in absolute and relative terms (less than 1,000 sq. km., or 0.02% of all African protected areas). There are two interesting exceptions to this regional pattern when one considers the amount of encroachment by both region and WDPA class: North America emerges as the best protector of *IUCN-high* areas and by far the worst protector of *non-IUCN* areas, and the Asia and Oceania region fares almost as poorly as Europe in protecting *IUCN-high* areas.

[Figure 8, about here]

[Table 5, about here]

3.2 Urban proximity

In this section, we turn our attention to those protected areas which are not already part of the built environment, but which still face risks due to their urban proximity. To calculate urban proximity, we reproject all of the conservation and urban maps into a Goode's Homolosine equal-area projection. We then estimate the distance from each pixel of protected land and the nearest pixel of urban, where we consider only those contiguous urban patches that are at least 2.5 sq. km in size (10 pixels). This filter eliminates small patches of urban speckle which are unlikely to either significantly alter their surrounding ecosystem or form the basis of future urban incursions. The solid colored lines in Figure 9 depicts the global distribution of urban proximate protected areas for the *IUCN-high* (red), *IUCN-low* (blue), and *non-IUCN* (grey) classes.¹³ There are three features of these curves with direct relevance to the degree of urban exposure faced by protected areas:

- (1) skewness of the curve—modal peaks which are closer to the right side of the plot are further from urban areas, reducing their exposure to urban-proximate risks,
- (2) height of the y-axis intercept—higher intercepts correspond to protected areas that will be immediately impacted by small amounts of urban expansion,
- (3) range of the initial plateau—the longer the initial level-sloped region persists prior to the steep ascent to the modal peak, the more resilient a protected area class is to moderate levels of urban expansion.

In examining the three WDPA classes from Figure 9 for these salient features, it becomes clear that globally, the *IUCN-high* and *non-IUCN* protected areas (red and dark-

¹³ The area under these density curves is equal to the total size of each WDPA class, but because the x-axis is on a log scale, it is difficult to make direct areal comparisons.

gray curves, respectively) are less urban-proximate and significantly more resilient to urban expansion than the *IUCN-low* protected areas (blue curve). The *IUCN-high* and *non-IUCN* curves have a modal peak that is more distant from urban than *IUCN-low* curve, and the plateaus of both curves are roughly one-third as high as *IUCN-low*. With respect to the third feature, the range of the initial plateau, all three WDPA classes are similar; their exposure to urban-proximity increases at about 5 km range.

[Figure 9, about here]

Urban-related risks faced by protected areas come in at least two forms: (1) indirect, through the alterations to ecosystem function wrought by large urban settlements, or (2) direct, through future urban encroachment. In the case of indirect impacts, the most important factor is the urban proximity and accessibility of protected areas. However, in the case of direct encroachment, the urban-suitability of the protected area can be as important a factor as urban-proximity. The global-scale characterization of urban suitability is well beyond the scope of this research, but as a first proxy, we have examined the role of average slope as a limiting factor in urban expansion. When the full MOD500 urban map is intersected with a global database of slope (GTOPO30),¹⁴ we find that 99% of all urban areas occur on land that has a mean slope of less than 7%. For those protected areas with slopes of 7% or more, it is unlikely that they will experience urban encroachment. Of course, this does not mean that urban encroachment never occurs on such land, or that these high slope areas are invulnerable to other land use

¹⁴ GTOPO30 is a 30'' arc-second resolution global topographic map created by the US Geological Survey. Documentation and data are available at <http://edc.usgs.gov/products/elevation/gtopo30/>.

change events such as logging or mining. The dashed curves in Figure 9 describe the urban-proximity or low-slope land (less than 7%) within each of the WDPA-classes. The main observations are that high slope ‘protects’ a larger absolute and relative amount of *IUCN-high* and *IUCN-low* areas than *non-IUCN* areas, and that this high slope protection is a more important factor for protected lands that are far from urban areas (10-50 km range) than for those that are closer to urban areas (1-5 km range).

To understand the geographic distribution of urban proximity within the WDPA system, the same analysis behind Figure 9 can be disaggregated by continental region (Figure 10). The colors and line-types from Figure 10 are the same as in Figure 9. Using the same three curve features from the analysis of Figure 9, it is evident that Africa is the continent with protected areas that are ‘safest’ from the risks of urban-proximity—relative to all of the other continents, the Africa y-intercept is by far the lowest, the plateau lasts the longest, and all three WDPA classes are skewed furthest to the right. North America and Latin America and the Caribbean are also in favorable situations with respect to these three features, followed by Asia and Oceania. Europe’s *IUCN-low* land stands out as a uniquely exposed class, with by far the largest y-intercept. Across most of the five continental regions, the *IUCN-high* lands are skewed more distant from urban areas than the *IUCN-low* and *non-IUCN* areas. As in the global plot, the level of protection afforded by high-slope land is most important in the 10-50 km range. Here, Africa is an important outlier; there is virtually no difference between the solid and dashed curves for this continent.

[Figure 10, about here]

4. MODEL FOR URBAN EXPANSION AND RESULTS

One of the primary risks faced by urban-proximate protected areas is the potential for future urban incursion. To date, there are no global-scale, moderate-resolution models of urban expansion. In this section, we introduce a methodology for converting existing country-level models of urban demographic change into estimates of urban extent on a 500 m-resolution grid (Section 4.1). This simple model allows us to generate urban expansion envelopes on decadal timescales from 2010-2100. We intersect these envelopes with the WDPA, and explore the implications of urban expansion for the world's protected areas at global and regional scales (Section 4.2).

4.1 Model description

For country-level estimates of urban population and economic output through 2100, we turn to the International Institute for Applied Systems Analysis (IIASA) national scenarios of demographic change (Grubler et al. 2007). IIASA's is one of four institutional-level downscaling projects (Gaffin et al. 2004; Bengtsson et al. 2007; van Vuuren et al. 2007) aimed at increasing the spatial resolution of the regional-level IPCC Special Report on Emissions Scenarios (SRES; Nakicenovic and Swart 2000; Van Vuuren et al. 2006). We choose Grubler et al. because they use a probabilistic population projection method (Lutz 1996; Lutz et al. 2001), they model urban and rural populations separately, and they update all of the SRES scenarios based on the results of the 2000 censuses. Grubler et al. explore three of the four SRES demographic and economic storylines (Table 6). Their modifications to these scenarios are discussed more completely in Riahi et al. (2007). Collectively, these three scenarios are designed to

encompass a wide range of alternate futures regarding demographic transition and changes in the world economy.

[Table 6, about here]

The four SRES downscaling projects also conduct a second stage of sub-national modeling, downscaling from their country-level results to global grids of between 30 km and 60 km in spatial resolution (measured at the equator). Grubler et al. (2007) generate a global 30' arc-minute grid (60 km cells) of urban and rural population density and gross domestic product. This grid is far too coarse for the 500 m resolution conservation maps we are analyzing, and we choose not to use these IIASA grids as the basis for our finer-resolution downsampling. In order to allocate urban and rural populations, the IIASA team used a combination of Gridded Population of the World (GPW), Digital Chart of the World (we refer to this map as Vector Map Level Zero, VMAP0), and NOAA's nighttime lights data dataset (Grubler et al. 2007). This overall approach is closely related to that of the Global Urban Rural Mapping Project (Table 2), which is constructed by the same group that produces GPW. In Section 2, we demonstrated some of the significant drawbacks of both GRUMP (overestimation) and VMAP0 (underestimation) relative to other, newer global urban maps (MOD500 and IMPSA). There are similar concerns with the sub-national downscaling efforts of the other three projects.

By conducting our own sub-national downscaling, we are able to draw on the global urban map which is most closely correlated with accuracy-assessed medium resolution maps—MOD500. Like all of the SRES downscaling efforts, our algorithm

makes a number of simplifying assumptions with respect to urban population density and the spatial form of urban expansion (Figure 11). We begin with the country-level SRES urban population estimates from IIASA (upper left corner of Figure 11), linking each country in the IIASA model with the countries of the MOD500 urban map.¹⁵ We then use the MOD500 urban map to estimate the amount of urban area within each country circa-2000. The number of urban residents in a given country divided by the urban area within that country yields the mean urban population density for the country (step one, Figure 11). Although there are indications that both developing and developed countries are experiencing a steady decline in urban density (Angel et al. 2005; Schneider and Woodcock 2006), we make the simplifying assumption that the urban density estimated from 2000 remains constant over time. Our model is conservative; even small decreases in mean urban density would significantly increase total global urban expansion.

[Figure 11, about here]

In step two, for each decade of the IIASA projection, we estimate the increase in each country's urban residents (numerator in lower middle of Figure 11). We then divide this increment by the country's population density from step one, yielding an estimate of the increase in urban area during that decade. For those counties where the urban population decreases (Europe, Japan, etc.), we do not model urban contraction, instead we keep the amount of urban land constant at the level of the previous decade (zero

¹⁵ There are 38 small island nations and territories that are not tracked in the IIASA method, but are mapped by MOD500 and described in our international boundary file. For these counties, we rely on UN median urban population projections through 2030. Beyond 2030, we make the conservative assumption that these populations remain static. In 2000, the total urban area of these islands represents only 0.06% of the MODIS 500 m urban map.

increase). This is a reasonable simplification when one considers that urban land is rarely converted back into natural vegetation, even when that urban land becomes uninhabited.

Steps one and two produce a decadal estimate of the amount of new urban land within each country. The remaining task is to design an algorithm for allocating this new urban land to the previous year's urban map (step three). We begin by masking out water pixels based on the LandScan 2006 land-water boundary, and eliminating high slope pixels ($> 6\%$) based on our GTOPO30 global topographic map. Next, we assume that urban expansion is most likely to occur near existing patches of urban area that are of sufficient size. As in Section 3.2, we eliminate all urban patches that are smaller than 2.5 sq. km. Finally, we rank all of the urban-suitable pixels within each country based on urban proximity and suitability, and select enough highly-proximate pixels to meet the decadal urban expansion requirements from step two. The same process is repeated for all 223 countries and the nine decadal increments from 2000-2100. There is a considerable literature surrounding the modeling of urban expansion at the grid-level, and most of these models rely on urban proximity in one form or another (Herold et al. 2003). Our decision to use an untransformed measure of urban proximity as our primary predictor of growth is in keeping with our desire to build a simple model.

4.2 Model results

Figure 12a plots the cumulative total of urban expansion from 2000-2100 under the three IIASA-SRES storylines. Through 2020, all three scenarios are essentially in agreement; A2 is only 5.3% greater than B1 in 2020. Urban areas expand by 260,000 sq.

km by 2020, an increase of 40% over the circa-2000 MOD500 area of 660,000 sq. km. Over the next ten years the spread between A2 and B1 opens to 14.5%, and from 2030 forward the three scenarios become quite distinct. By 2100, the mean cumulative urban expansion for all three scenarios is 637,000 sq. km—roughly a doubling of circa-2000 urban extent.

[Figures 12a, 12b, and 12c, about here]

When we turn to the question of projected area losses (Figure 12b), it is important to recall that an assumption of our model is that protected areas completely lack enforcement. In allocating urban expansion (step three, Figure 11), the protection status of a pixel has no impact on whether than pixel is reclassified as new urban. Although for convenience we refer to ‘losses’ of protected area, our estimates can more conservatively be thought of as proxies for the amount of human-induced pressure faced by the existing protected area network and the amount of effort that may be required to keep the network urban-free.

The overall pattern for losses of protected areas follows a similar trajectory as that of overall urban expansion, albeit on a much smaller scale. Figure 12b plots the envelopes of future protected area losses for the three main classes from 2000-2100. The upper edge of the shaded areas is modeled with A2 population data, the lower edge with B1 data, and the solid line with B2 data. As in Figure 12a, the three storylines are in rough agreement through 2030, indicating a total loss of protected areas of 17,400 sq. km (mean of three scenarios)—nearly double the circa-2000 urban incursions and inholdings

reported in Figure 8 (Section 3.1). Overall, the *IUCN-low* areas (blue) suffer the most from urban expansion, followed by *non-IUCN* areas, and *IUCN-high* areas.

Although the cumulative amount of protected area that is lost increases steadily throughout the century, for scenarios A2 and B2 the share of overall urban expansion attributed to protected areas decreases from roughly 5% to 3.5% by 2060, and increases slightly thereafter (Figure 12c). For the B1 scenario, the percent of decadal urban expansion that occurs on protected areas increases sharply starting in 2070. The source of this divergence from the other scenarios remains an open question.

There is a high degree of geographic variation in the distribution of these protected area losses. The bar-plots of Figure 13 describe the cumulative regional losses by protected area class for three dates: 2030, 2060, and 2090. The population model underlying these results was the median, B2, model. Because of its projected decline in population, Europe faces the least amount of protected area losses. North America and Latin America and the Caribbean face similar amounts of total loss, but the composition is quite different, with the majority of the North American losses in *non-IUCN* land and the majority of Latin America and the Caribbean losses in *IUCN-low* land. The Africa and Asia regions are in a class of their own, with rapid increases in the total amount of protected area losses and far more losses in the critical *IUCN-high* areas. Through 2100, across all three protected area groups, the B2 scenario estimates more than 30,000 sq. km of losses globally, more than double the current amount of incursion and inholdings mapped by the MODIS 500 m map. Together, the Asia and Oceania and the Africa regions account for 58.7% of this total.

5. FUTURE DIRECTIONS

The model results from Section 4 are intended as a first glimpse of the important role that may be played by global urban expansion in the future of the global network of protected areas. This is an ongoing research effort, with a considerable number of opportunities for improvement. This section is a chance to reflect on some of the limitations of the current work, and to discuss future research directions. The section is organized in the same way as the larger paper, beginning with the selection of a single global urban map (Section 2), followed by the spatial analysis of urban and protected areas (Section 3), and finally, models of urban expansion (Section 4).

Several limitations of the map assessment in Section 2 have already been mentioned, including concerns regarding the adequacy of the 120 assessment cities. We are working to expand the validation data by one-third through using circa-2000 Landsat maps from Schneider and Woodcock (2006). In addition, a new Google Earth land cover assessment tool may prove helpful in extending our validation to cities of less than 100,000 residents.¹⁶ The overall strategy in Section 2 was to select a single ‘best’ map of urban areas. An alternative to this approach is to capture the information content of several maps through the use of map fusion techniques. In this approach, the Landsat city maps would be used as training data and the global urban maps as input data for a supervised classification of urban areas. Random forest regression trees may be uniquely well-suited for this task (Breiman 2001). Global urban map fusion is the subject of ongoing research.

¹⁶ Separate research has proven that the high resolution imagery within the Google Earth archive is geo-located with sufficient accuracy for assessing Landsat-resolution imagery (Potere in preparation).

In Section 3, we highlighted the fact that those pixels that are labeled as urban in MOD500 and protected in the WDPA may in fact be attributed to map errors. Only a visit to the site or recent high resolution imagery can resolve this uncertainty. As in the assessment work from Section 2, our web-based Google Earth land cover assessment tool may prove useful here. The concept is to build a stratified random sample of overlap pixels, and visit them using high resolution imagery on Google Earth. Thus far, more than 90% of our 120 assessment cities are covered by high resolution imagery (Figure 3), and the Google Earth archive is constantly expanding. If the base of sample sites is of adequate size, this assessment work would allow us to place confidence limits on the estimates of current urban incursions and inholdings. The approach has the potential to identify important instances of illicit activities within protected areas.

The urban expansion model of Section 4 is a recent development, and there are a wide range of ongoing improvement efforts which extend to all aspects of the algorithm (Figure 11). As mentioned earlier, the assumption that urban density remains static in time is strong. By relaxing this assumption, Angel et al. (2005) made an aspatial estimation that urban areas in the developing world could triple by 2030. Perhaps in part because we assume constant urban density, a tripling does not occur in our models until 2100 in the A2 scenario. One potential improvement that we are exploring is to construct a regional model of urban density by drawing on the gross domestic product data from the same Grubler et al. (2007) SRES model that supplies our population time series. From Figure 14, it appears that there is a reasonably strong negative relationship between economic prosperity and urban density.

[Figure 14, about here]

There are several model improvements related to step three (Figure 11), the spatial allocation of new urban pixels. On the subject of data quality, there are new global datasets for topography and the land-water boundary that are of higher resolution and better quality than those employed thus far. We are in the process of aggregating the Shuttle Radar Topography Mission (SRTM) gap-filled dataset from 90m to 500m.¹⁷ This new slope data will allow us to constrain urban growth at the country level, instead of relying on a single global limit of 6% slope.

Our 160-city database of Landsat maps contains maps for both 1990 and 2000. Because they encompass two dates, these maps could prove quite valuable for designing a more nuanced model of urban expansion than the basic proximity model now employed. The Grubler et al. (2007) group used a gravity model for their expansion algorithm, which allows one to consider not only the distance to the nearest urban area, but also the amount of urban land within the local neighborhood of a given pixel. An improved model of urban expansion could also consider the land cover class of the non-urban pixel, building separate transition probabilities for each class. Our Landsat assessment archive, when aggregated to the same resolution as MODIS, could provide the basis for tuning these various model parameters.

The final area of potential improvement is most closely related to the core conservation questions which motivate this project. We make the assumption in our urban expansion model that protected areas are completely without enforcement. It is

¹⁷ The SRTM dataset is produced by the Consultative Group for International Agriculture Research (CGIAR) Consortium for Spatial Information (CSI) <http://srtm.csi.cgiar.org/>.

possible to modify this assumption, allowing protected areas to resist urban encroachment. This resistance could be set in a binary fashion or continuously. By inserting the effectiveness of protected areas into the model, it will be possible to test a wide range of global-scale conservation strategies. For example, should conservation managers could focus most on those parks that contain the most threatened species, on those parks that face the most pressure from human-related activities, or on those that are the most pristine? There is little doubt that urbanization will alter the distribution of land suitable for future conservation preserves; modeling those alterations is the most reasonable way to improve our ability to identify and acquire high-priority reserve sites before they urbanize.

TABLES AND FIGURES (in order of appearance)

IUCN categories	Purpose / Size (sq. km) / percent of all protected areas
Category Ia	<p>Strict nature reserve: protected area managed mainly for science. (744,000) (4%)</p> <p>Definition: Area of land and/or sea possessing some outstanding or representative ecosystems, geological or physiological features and/or species, available primarily for scientific research and/or environmental monitoring.</p>
Category Ib	<p>Wilderness area: protected area mainly for wilderness protection. (322,000) (2%)</p> <p>Definition: Large area of unmodified or slightly modified land, and/or sea, retaining its natural character and influence, without permanent or significant habitation, which is protected and managed so as to preserve its natural condition.</p>
Category II	<p>National park: protected area managed mainly for ecosystem protection and recreation. (3,853,000) (23%)</p> <p>Definition: Natural area of land and/or sea, designated to (a) protect the ecological integrity of one or more ecosystems for present and future generations, (b) exclude exploitation or occupation inimical to the purposes of designation of the area and (c) provide a foundation for spiritual, scientific, educational, recreational and visitor opportunities, all of which must be environmentally and culturally compatible.</p>
Category III	<p>Natural Monument: protected area managed mainly for conservation of specific natural features. (172,000) (1%)</p> <p>Definition: Area containing one, or more, specific natural or natural/cultural feature which is of outstanding or unique value because of its inherent rarity, representative or aesthetic qualities or cultural significance.</p>
Category IV	<p>Habitat/species management area: protected area managed mainly for conservation through management intervention. (2,463,000) (15%)</p> <p>Definition: Area of land and/or sea subject to active intervention for management purposes so as to ensure the maintenance of habitats and/or to meet the requirements of specific species.</p>
Category V	<p>Protected landscape/seascape: protected area managed mainly for landscape/seascape conservation and recreation. (2,213,000) (13%)</p> <p>Definition: Area of land, with coast and sea as appropriate, where the interaction of people and nature over time has produced an area of distinct character with significant aesthetic, ecological and/or cultural value, and often with high biological diversity. Safeguarding the integrity of this traditional interaction is vital to the protection, maintenance and evolution of such an area.</p>
Category VI	<p>Managed resource protected areas: protected areas managed mainly for the sustainable use of natural ecosystems. (3,280,000) (19%)</p> <p>Definition: Area containing predominantly unmodified natural systems, managed to ensure long term protection and maintenance of biological diversity, while providing at the same time a sustainable flow of natural products and services to meet community needs.</p>

Table 1, continued.

<i>Non-IUCN</i> categories	Purpose / Size (sq. km) / percent of all protected areas
National sites	(3,343,000) (20%) Definition: Protected areas designated by national governments which have not yet been classified according to the IUCN classification scheme.
World Heritage areas	(203,000) (1%) Definition: Sites significant to ‘world cultural and natural heritage.’ These sites are listed in the World Heritage Convention, which is administered by the United Nations Educational, Scientific and Cultural Organization (UNESCO) World Heritage Committee.
Ramsar wetlands	(239,000) (1%) Definition: Sites which belong to an international treaty for the protection of wetlands first signed in Ramsar, Iran, in 1972.
UNESCO Man and the Biosphere reserves	(11,000) (1%) Definition: Sites protected for research and training activities under the UNESCO MAB program.

Table 1 (previous page). Protected area classification system, according to the IUCN (1994), and Lockwood et al. (2006). The global sizes reported for each class are free of overlaps; each parcel of protected land can only belong to one category. Conflicts were resolved by assigning priority to sites with IUCN classification, then international treaty sites (World Heritage, Ramsar, or Man and the Biosphere), and lastly, national sites.

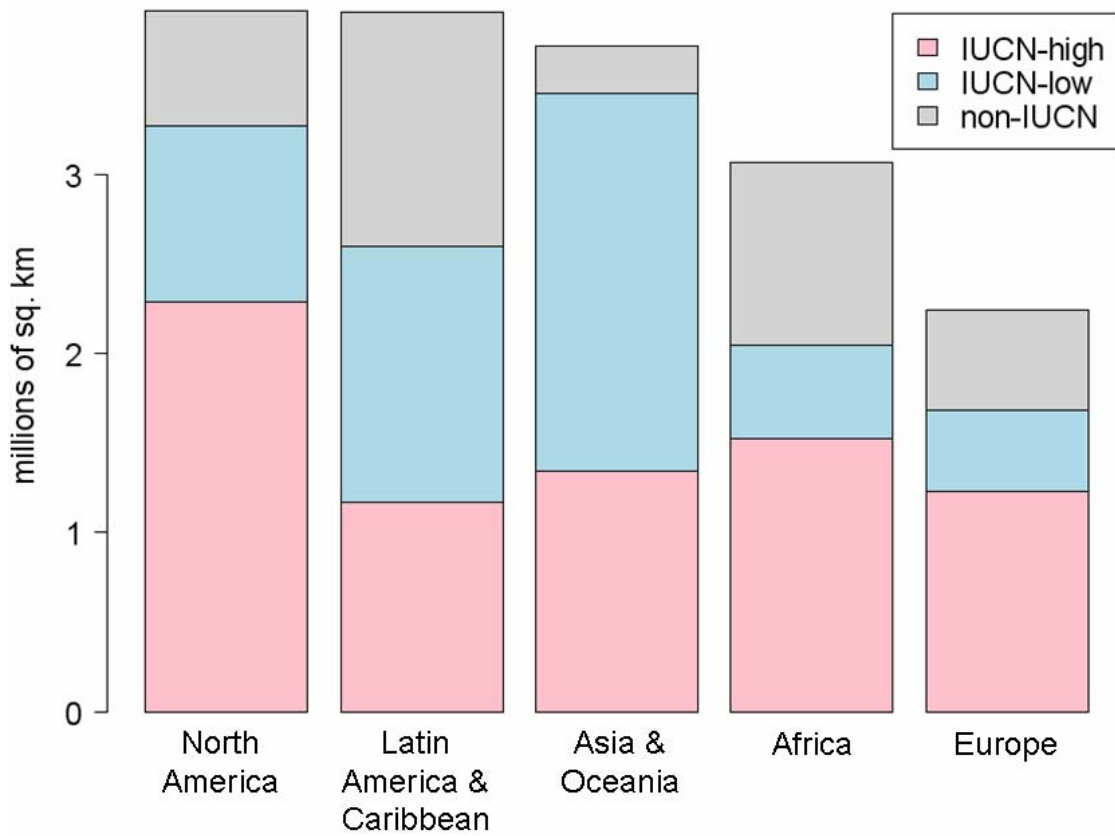


Figure 1. Regional distribution of protected areas. The global total for terrestrial protected areas in the 2007 World Database of Protected Areas map is 16.8 million sq. km. We consider only those protected areas that contain a spatially-explicit boundary in the WDPA.

Code	Map / paper	Producer	Specifications / Source
VMAPO	Vector Map Level Zero (Danko 1992)	US National Geospatial-Intelligence Agency	land cover and map features, vector, 1:1,000,000 scale, geographic projection, http://geoengine.nga.mil/
GLC00	Global Land Cover 2000 v1.1 (Bartholome et al. 2005)	European Commission Joint Research Center	land cover, 22 classes, raster, 32" arc-seconds (~1 km), geographic projection, http://www-gvm.jrc.it/glc2000/
HYDE3	History Database of the Global Environment v3 (Goldewijk 2005)	Netherlands Environmental Assessment Agency	global fraction of urban land, raster, 5' arc-minutes (~10 km), geographic projection, http://www.mnp.nl/hyde/
IMPASA	Global Impervious Surface Area (2000-2001) (Elvidge et al. 2007)	Earth Observation Group, US National Geophysical Data Center	global fraction of urban land, raster, 30" arc-seconds (~1 km), geographic projection, http://www.ngdc.noaa.gov/dmsp/
MOD500	MODIS Urban Land Cover 500 m (2001v5) (Schneider et al. forthcoming)	University of Wisconsin and Boston University (US-NASA)	global urban land, Raster, ~500 m resolution sinusoidal projection http://www.sage.wisc.edu
MOD1K	MODIS Urban Land Cover 1km (2001v4) (Schneider et al. 2003; 2005)	Boston University Department of Geography (US-NASA)	global urban land, raster, ~1km resolution, sinusoidal projection, http://www-modis.bu.edu/landcover/
GRUMP	Global Rural-Urban Mapping Project , alpha (CIESIN 2004)	Earth Institute at Columbia University	urban / rural map, raster, 30" arc-seconds (~1 km), geographic projection, http://sedac.ciesin.columbia.edu/gpw/
LITES	DMSP-OLS Nighttime Lights v2 (2001, F15 sat.) (NGDC 2007)	National Geophysical Data Center (US-NOAA)	nighttime illumination intensity, raster, 30" arc-seconds (~1km), geographic projection, http://www.ngdc.noaa.gov/dmsp/
LSCAN	LandScan 2005 (Bhaduri 2002)	US Oak Ridge National Laboratory (US-DOE)	ambient human population, raster, 30" arc-seconds (~1 km), geographic projection, http://www.ornl.gov/sci/landscan/

Abbreviations: DOE, Department of Energy; DMSP-OLS, Defense Meteorological Satellite Program-Operational Line Scanner; MODIS, Moderate Resolution Imaging Spectroradiometer; NASA, National Aeronautics and Space Administration; NOAA, National Oceanographic and Atmospheric Administration.

Table 2. The seven global urban maps examined in this research in order of increasing global urban extent, and two urban-related maps (bottom two rows).

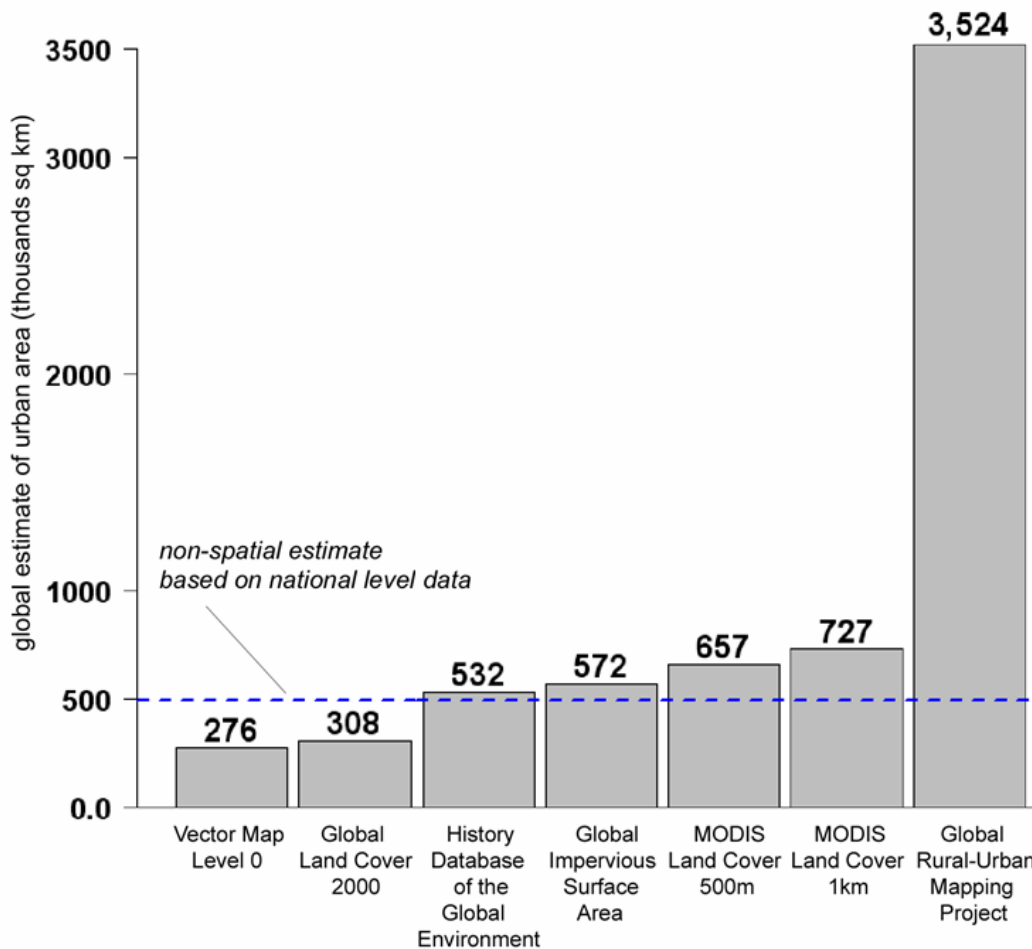


Figure 2. Global extents for seven spatially explicit estimates of urban area (thousands of sq. km): Vector Map Level Zero, Global Land Cover 2000 v1.1, History Database of the Global Environment v3, Nighttime Lights-based Global Impervious Surface Area beta product, Moderate Resolution Imaging Spectroradiometer (MODIS) 500m Urban Land Cover v5 2001, MODIS 1 km Urban Land Cover v4 2001, and Columbia University’s Global Rural-Urban Mapping Project version alpha. Above each bar is the estimate of global extent in thousands of sq. km. The dotted line is an estimate of urban area based on national-level urban statistics (UN 2005) and regional-level urban population densities for the year 2000 from Angel et al. (2005). Note the order of magnitude difference for these totals.

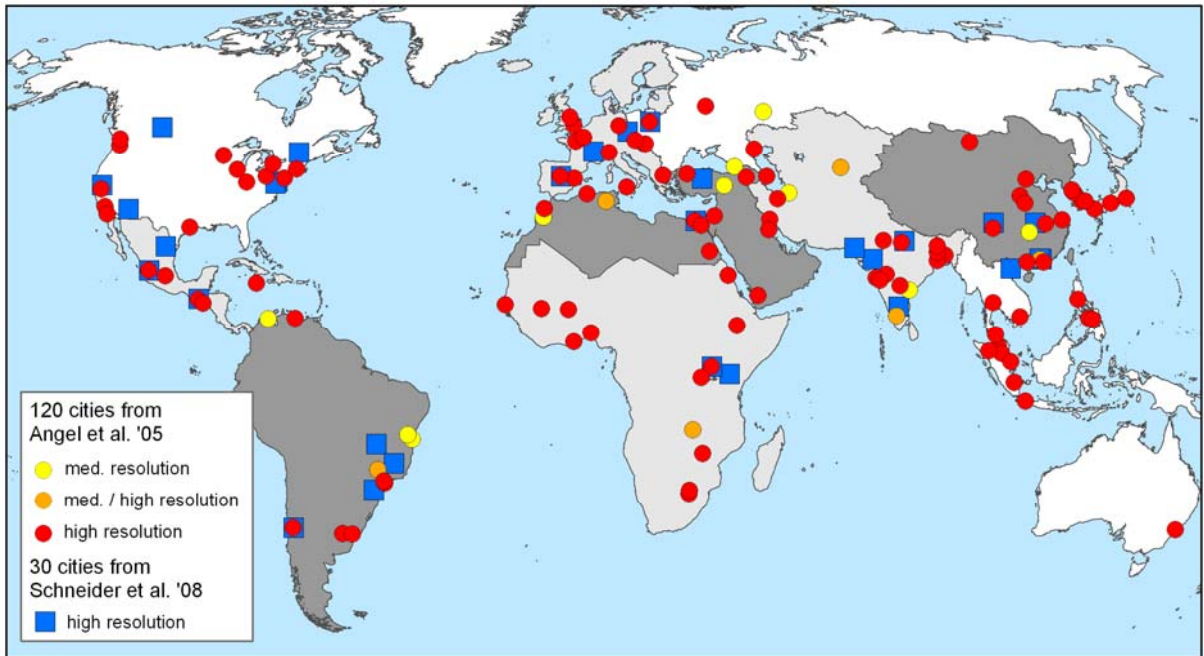


Figure 3. A global sample of cities greater than 100,000 from the Angel et al. (2005) study. The color of each city indicates the high and medium resolution imagery available in Google Earth as of February 2008.

City Name (Population 2000, x1000)	VMAPO	GLC00	HYDE3	IMPISA	MOD500	MOD1K	GRUMP	Regional Omission Rates
Zhengshou, China (2,070)		0						East Asia (56%) (9/16)
Yulin, China (1,558)	<5	0						
Leshan, China (1,373)	<5							
Yiyang, China (1,343)		0					<5	
Ulan Bator, Mongolia (738)			<5					
Changzhi, China (594)		0						
Anging, China (566)		0						
Chinju, Korea (287)		0						
Chonan, Korea (114)		<5						
Baku, Azerbaijan (1,936)		<5						W. Asia (63%) (5/8)
Sanaa, Yemen (1,653)		<5						
Yerevan, Armenia (1,407)		0						
Malata, Turkey (437)		0						
Zugdidi, Georgia (105)		<5						
Gorgan, Iran (189)		0						SC Asia (6%) (1/16)
Cebu, Philippines (719)						<5		SE Asia (8%) (1/12)
Vallendupar, Columbia (274)		0						Latin Am. (19%) (3/16)
Ilheus, Brazil (162)	0							SS Africa (17%) (2/12)
Jequie, Brazil (130)	0	<5						
Banjul, Gambia (399)	<5							
Kigali, Rwanda (351)	<5	0						N. Africa (25%) (2/8)
Port Sudan, Sudan (384)	<5	0					<5	
Tebessa, Algeria (163)	<5							
Fukuoka, Japan (1,341)		<5						ODC + Europe (3%) (1/32)
Total Omissions	8	18	1	0	0	1	2	
Omission Rate (120 cities)	7%	15%	1%	0%	0%	1%	2%	
	VMAPO	GLC00	HYDE3	IMPISA	MOD500	MOD1K	GRUMP	

Abbreviations: ODC, Other Developed Countries; SS Africa: Sub-Saharan Africa; SC Asia, South Central Asia.

Table 3. Omitted cities from a 120-city sample of cities greater than 100,000 in population (Angel et al. 2005). Zero's mark cities that were completely omitted by a global urban map, and '<5' marks cities that were mapped with less than 5 sq. km of urban land. To estimate omission rates, any city mapped as 5 sq. km or less was considered an omission. The rightmost entries track regional omission rates (across all maps). The bottom row tracks omission totals and rates for each map (across all regions). The number in parenthesis to the right of the city names is the population in the year 2000 (thousands). The regional scheme is from Angel et al. (2005).

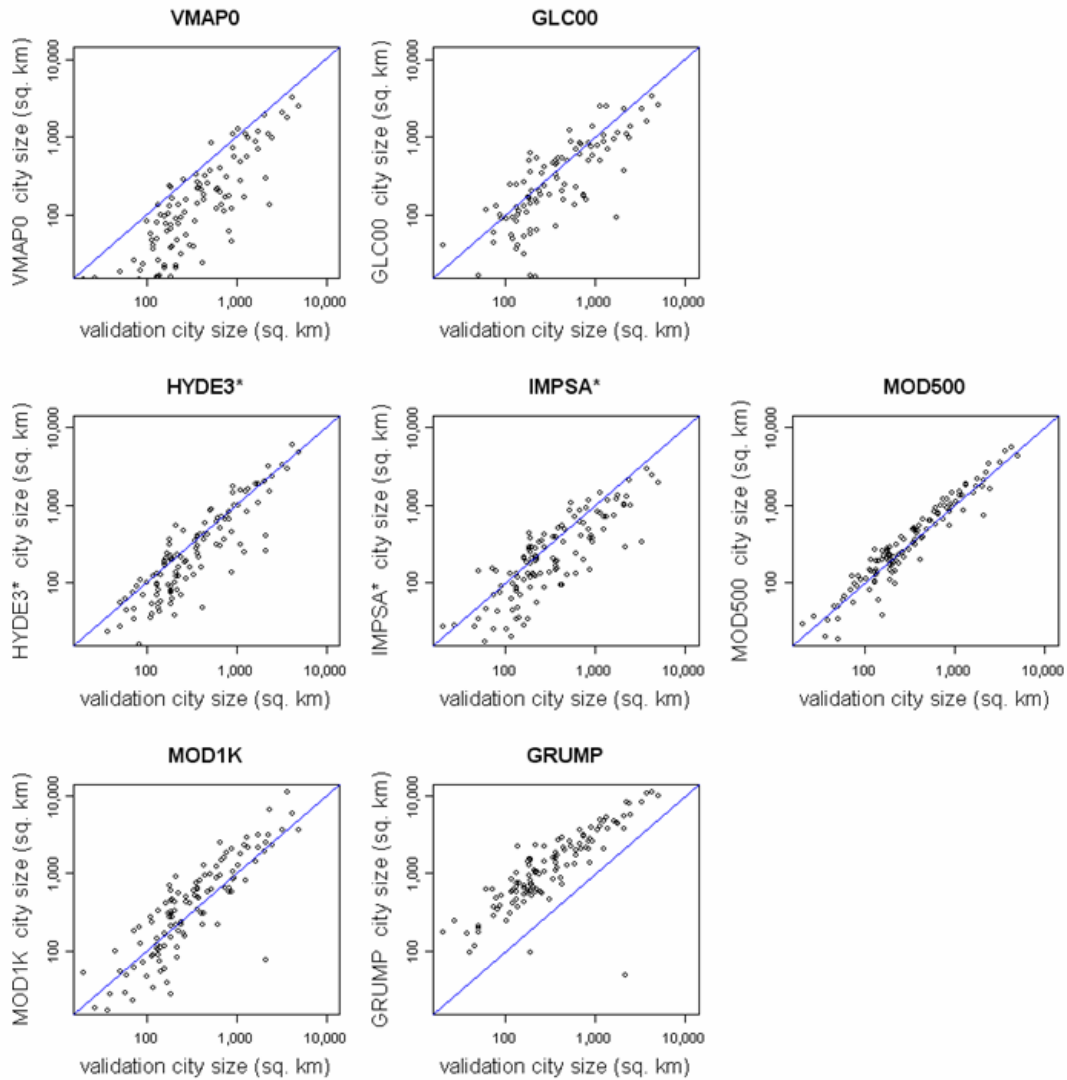


Figure 4. Scatter-plots of city size for the 120 cities within the Angel et al. (2005) sample (log-log scale). The plots describe the size in sq. km for each city according to the assessment maps (x-axis) versus the area mapped as urban for each of the seven global urban maps (y-axis). The blue lines indicate 1:1 agreement.

Contingency Table		Validation Data	
		Presence	Absence
$n = a + b + c + d$			
Data under Review	Presence	a	b
	Absence	c	d

Cohen's Kappa	$\frac{\left(\frac{a+d}{n}\right) - \frac{(a+b)(a+c) + (c+d)(d+b)}{n^2}}{1 - \frac{(a+b)(a+c) + (c+d)(d+b)}{n^2}}$
----------------------	--

Table 4. A typical contingency table for a two-class map comparison (top box). In the case of this work, presence is equivalent to urban, and absence to non-urban land. For the assessment, ‘data under review’ is the global urban map in question and ‘validation data’ is the medium resolution Landsat map. From the cells of this contingency matrix, it is possible to generate a large number of statistics designed to measure overall map agreement. The measure we report in Figure 5 is Cohen’s kappa (Cohen 1960; Congalton and Green 1999).

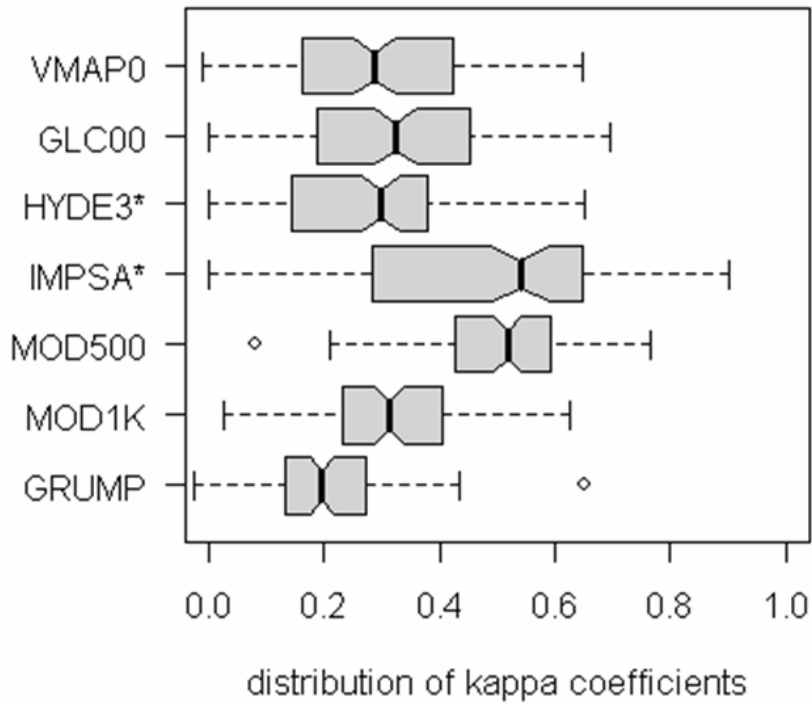
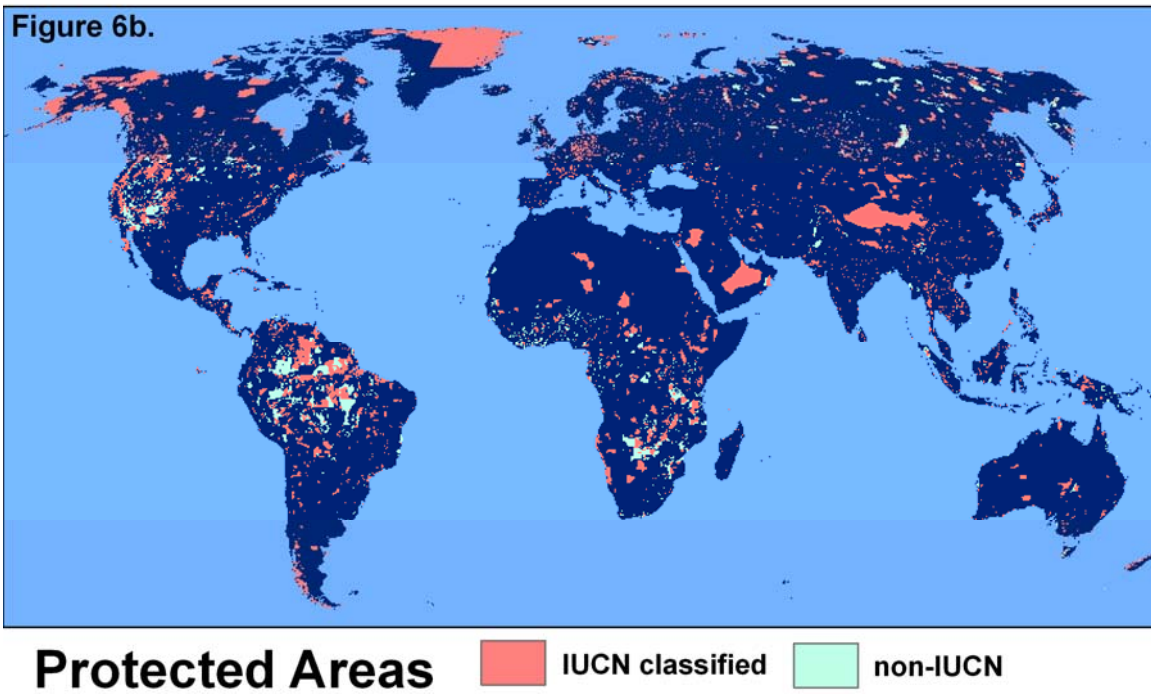
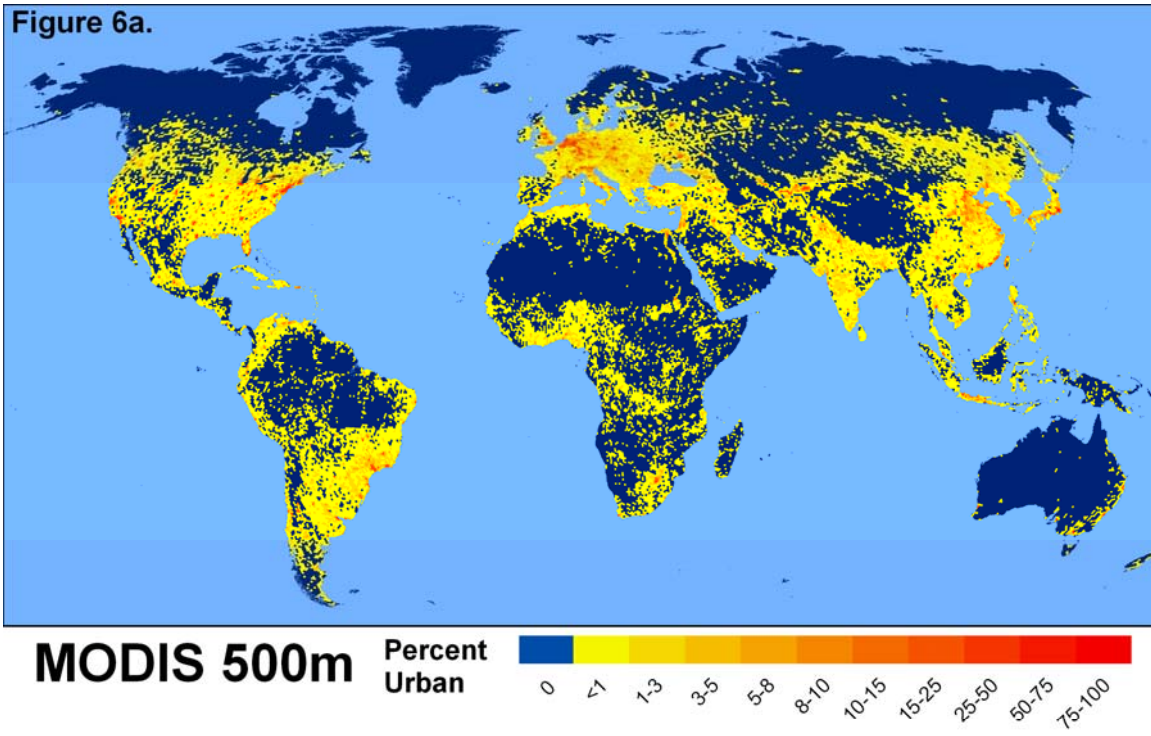


Figure 5. Map agreement statistics for each of the seven global urban maps. We constructed contingency tables for the 120 cities of the Angel et al. (2005) Dynamics of the Global Urban Expansion project, and then estimated Cohen’s kappa statistics for each. The box-plots describe the distribution of kappa values for each global urban map, values of 1.0 indicate perfect agreement. The asterisks adjacent to HYDE3 and IMPSA indicate that we used a thresholded version of those maps, where majority urban pixels ($\geq 50\%$ impervious surface) were labeled as urban and all others as non-urban.



Figures 6a and 6b. The global distribution of urban areas (6a) and protected areas (6b) according to the MODIS 500 m global urban map and the World Database of Protected Areas, respectively.

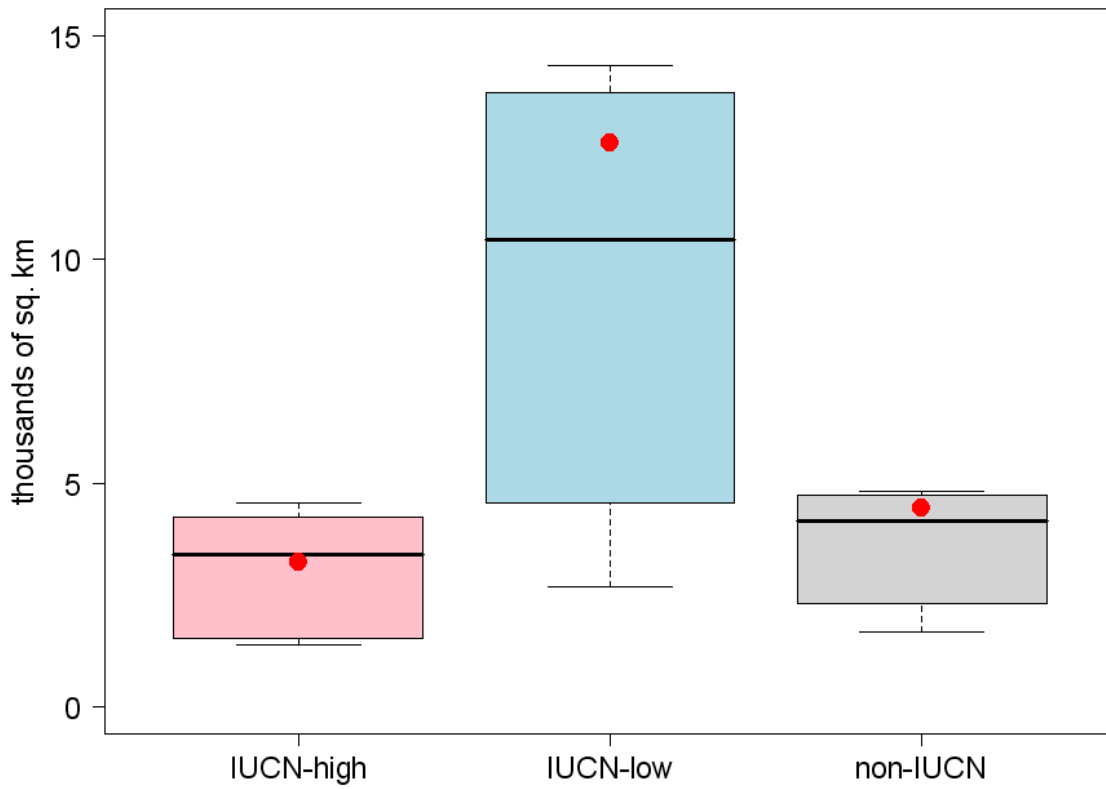


Figure 7. The area of overlap between seven global urban maps, and the World Database of Protected Areas. The red dot marks the overlap for the MODIS 500 m map.

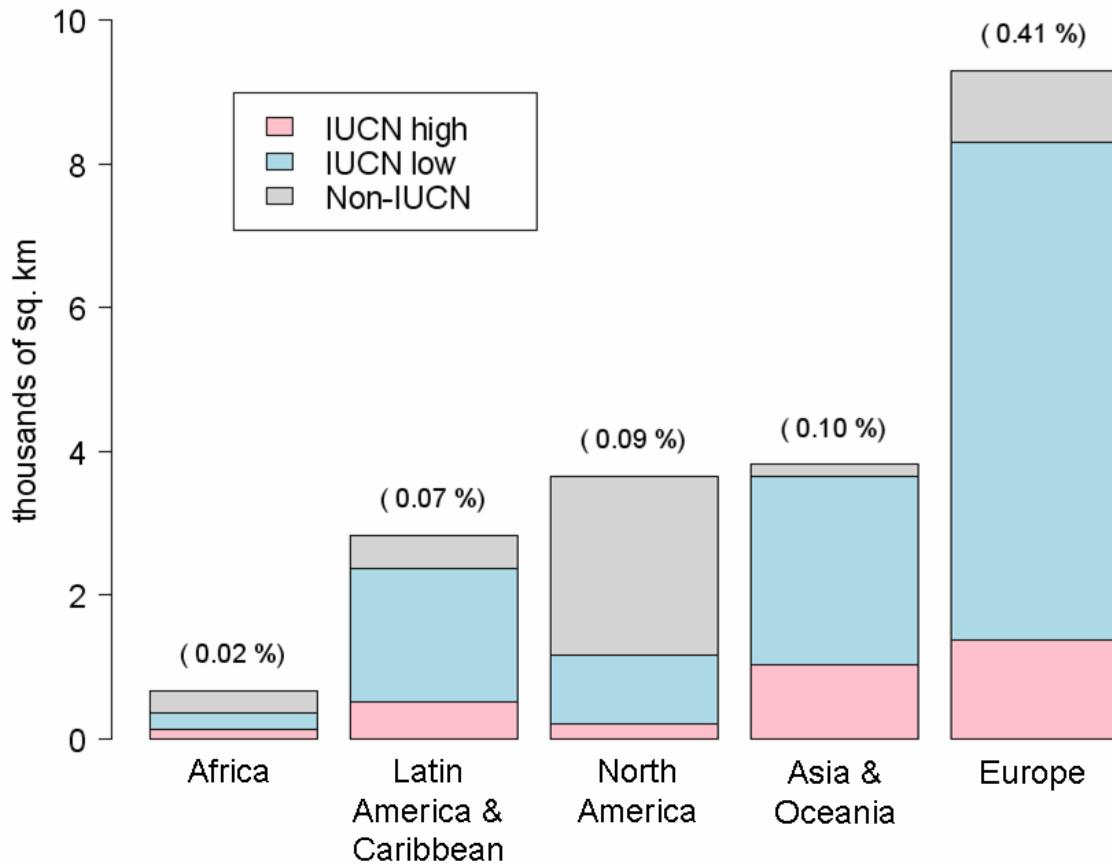


Figure 8. The regional distribution of land that is mapped as both *urban* in the MODIS 500 m global map and *protected* by the World Database of Protected Areas. The percentages above each regional bar express the total overlap area as a percentage of all protected areas within that region. The regional scheme is from the UN Statistics Division.

	IUCN Ia-IV			IUCN V-VI				Non-IUCN				<i>total</i>
	Ia	Ib	II	III	IV	V	VI	Ram.	WHS	MAB	Nat.	
North America, Australia & New Zealand	2	3	26	28	159	374	580	45	7	0	2,457	3,682
Western Europe & Japan	1	161	296	30	424	7,346	0	212	3	7	297	8,777
Eastern Europe	39	4	154	28	522	238	2	75	298	0	115	1,474
Central America & Caribbean	0	0	43	3	10	17	51	2	0	0	45	171
South America	22	0	375	22	35	1,664	175	128	176	0	128	2,726
Sub-Saharan Africa	1	0	73	0	53	6	177	21	6	0	283	620
Western Asia & North Africa	6	0	8	0	11	48	185	8	0	0	9	275
South Central Asia	17	0	199	0	315	33	0	13	0	1	74	651
East Asia	3	2	9	5	2	1,200	524	2	18	0	1	1,764
Southeast Asia & Pacific Islands	54	1	63	32	57	68	24	1	1	3	36	338
<i>total</i>	146	170	1,245	148	1,587	10,994	1,720	507	508	11	3,444	20,479

Table 5. The regional distribution of land that is mapped as urban in the MODIS 500 m global map and as protected by the World Database of Protected Areas. The world regional scheme differs from Figure 8; the ten world regions are a slightly modified version of the UN regional scheme (discussed more fully in Potere and Schneider 2007).

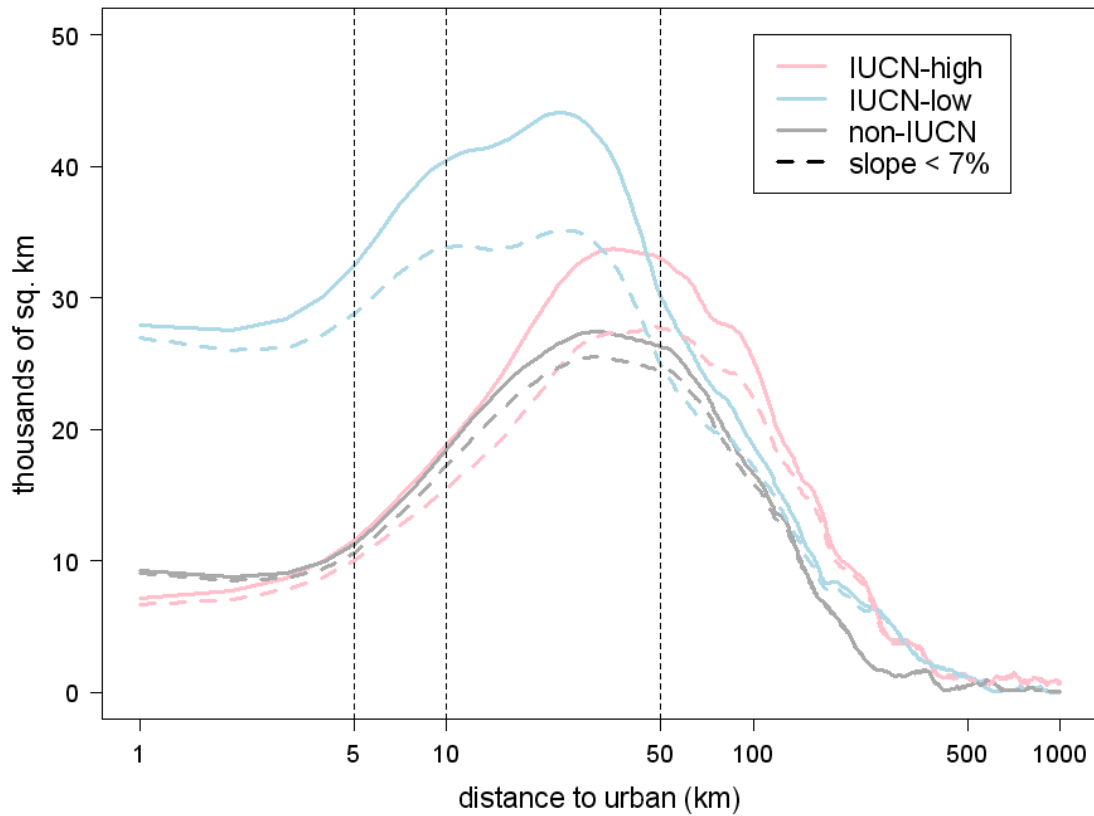


Figure 9. The urban-proximity distributions for three classes of protected areas. The solid lines describe the urban proximity distribution for all protected areas, and the dashed lines are for those protected areas with an average slope of less than seven degrees. The y-axis is on a logarithmic scale (dotted lines at 5,10, and 50 km are intended to facilitate interpretation). The y-intercept includes urban inholdings and incursions. Estimates are based on the MODIS 500m urban map (MOD500) and the World Database of Protected Areas (WDPA).

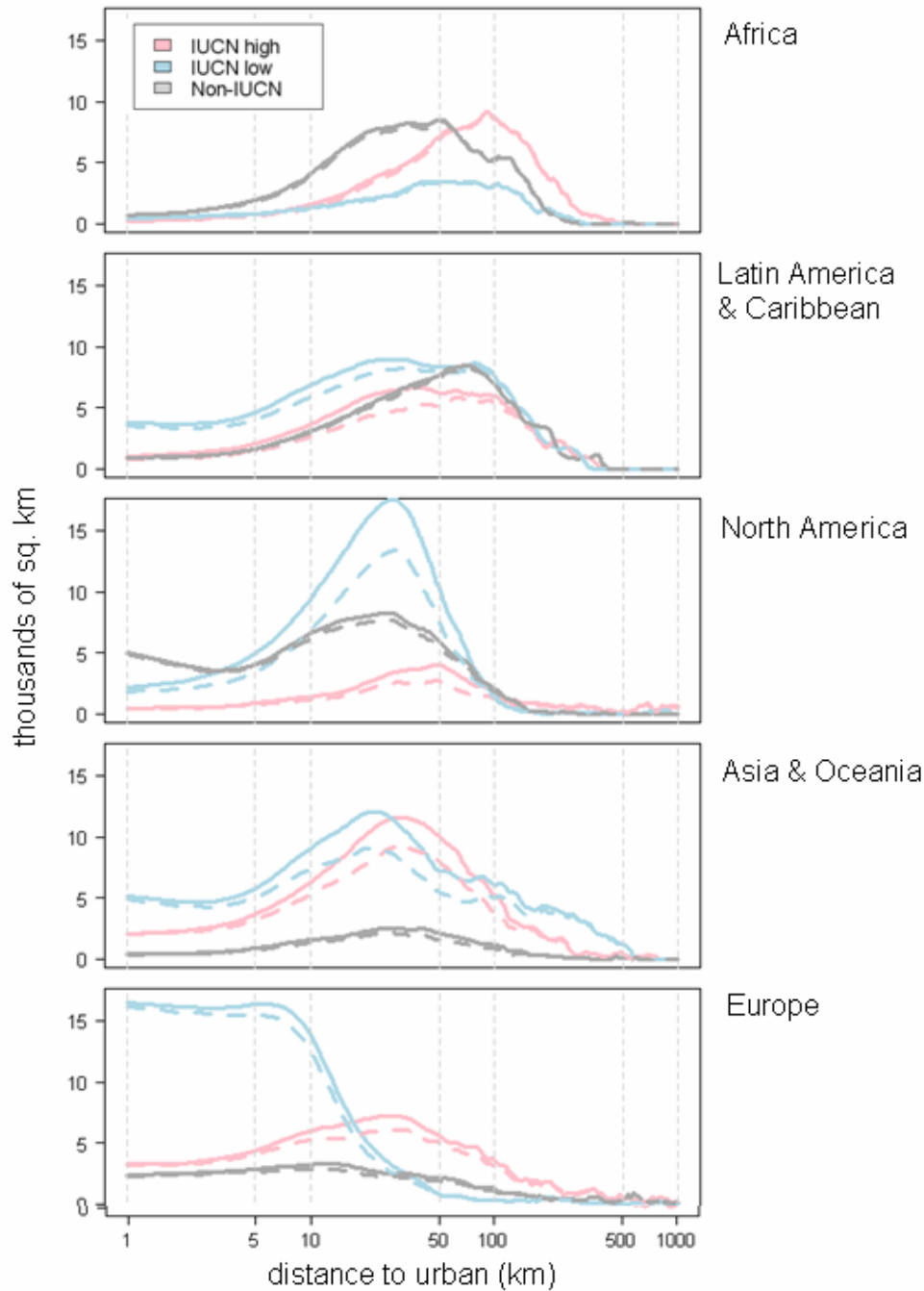


Figure 10. Distributions of urban proximity for three classes of protected area, across five world regions. As in Figure 9, the dashed lines are for low slope (less than 7%) protected areas. By region, the median urban distance for all protected land within 100 km of urban areas is (from top to bottom in Figure 10): 32, 30, 28, 28 and 18 km.

	A2r	B2	B1
<i>Population</i>			
Population size	High	Medium-high	Low
Demographic transition	Delayed and slow	Medium	Rapid
Long-term fertility levels	Near or below replacement	Converging to replacement	Well below replacement
<i>Urbanization</i>			
Urbanization rates	High	Medium	Low
Megacity growth	High	Localized (Asia)	Low (constrained)
Urban-rural gradient	Medium-high	Medium	Converging to zero
<i>Income</i>			
Income growth	Medium-low	Medium	High
Income convergence	Very low (initially diverging)	Medium-low	Very rapid
Domestic/International price differences	Initially persistent, slow convergence after 2040	Medium convergence (linked to labor productivity)	Rapid convergence

Table 6. IPCC-SRES scenarios (storylines). From Grubler et al (2007), the three modified Intergovernmental Panel on Climate Change (IPCC) Special Report on Emissions Scenarios (SRES) storylines used by the IIASA downscaling team. From here forward, we use A2r and A2 interchangeably.

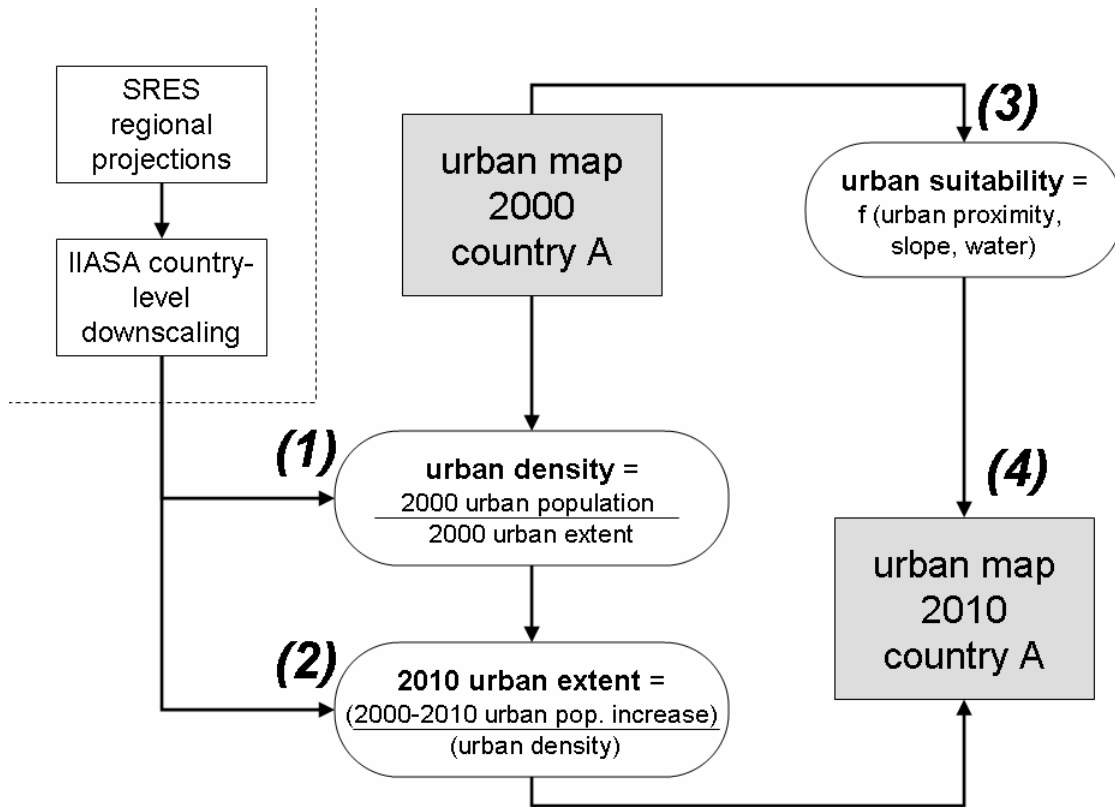


Figure 11. Model of global urban expansion. The principal inputs are the SRES storylines from IIASA (Grubler et al. 2007), and the MODIS 500 m urban map (Schneider et al. in preparation).

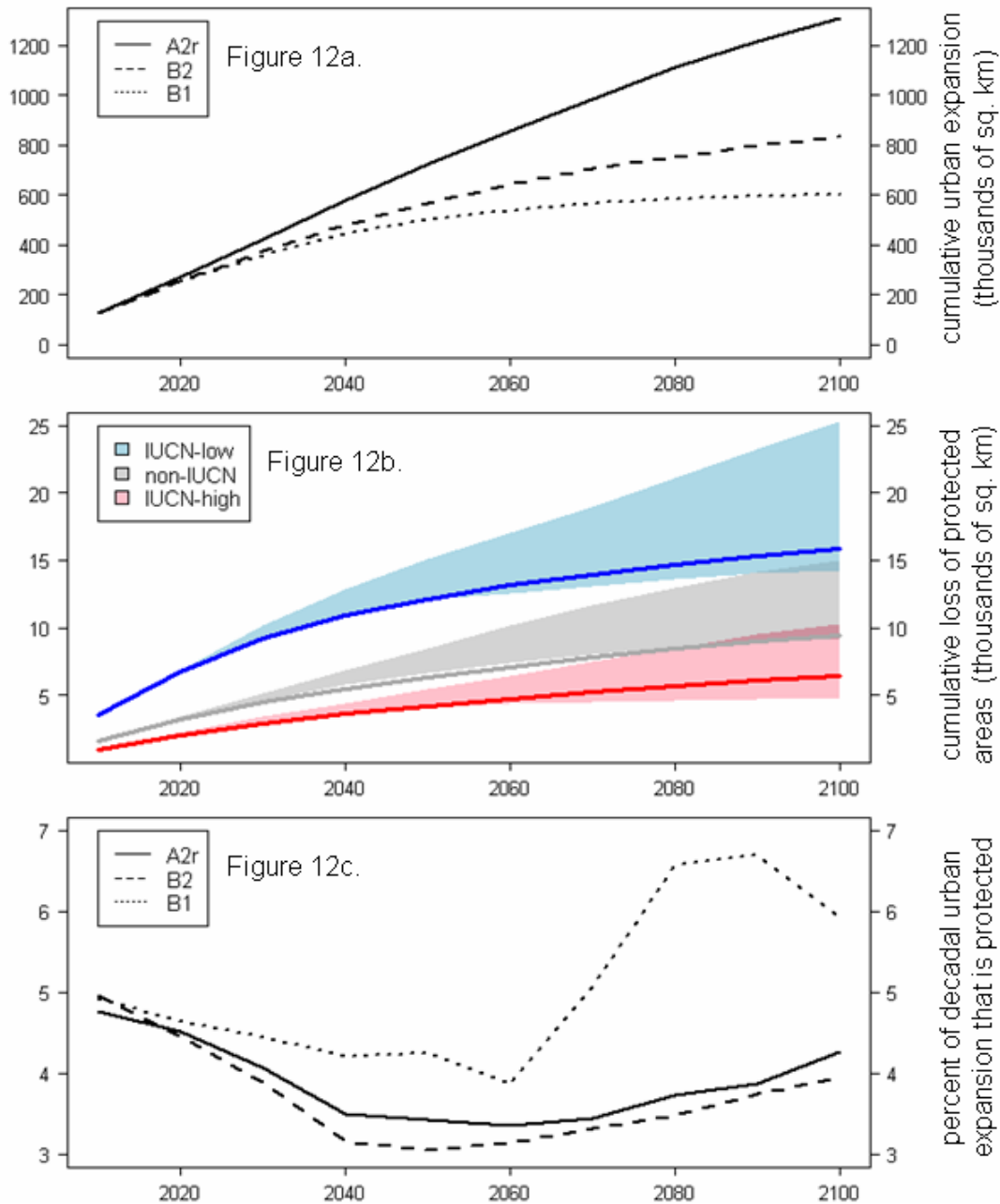


Figure 12abc. Model estimates of total urban expansion (top), total protected area losses (middle), and the percent of each decade’s urban expansion that is protected land (bottom). All plots span the years 2010 through 2100 (y-axis), and consider all three SRES scenarios. For Figure 12b, the shaded bocks are bracketed by scenario A2r (upper bound) and B1 (lower bound), and the solid lines mark the B2 median scenario.

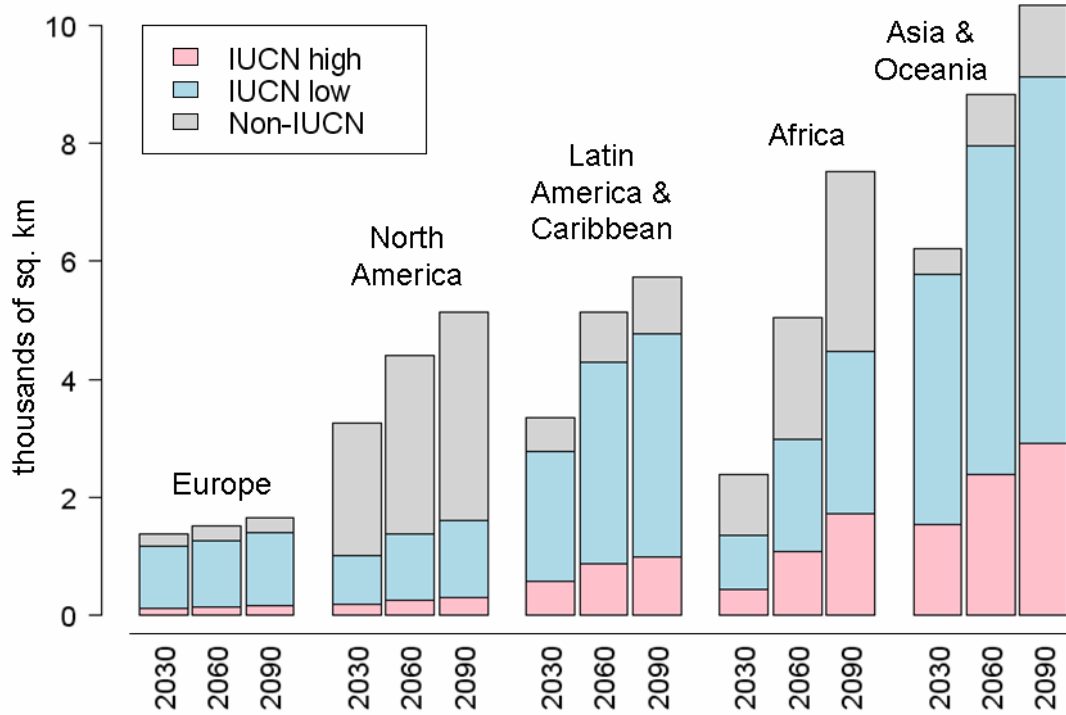


Figure 13. Model estimates of cumulative losses in protected areas for the years 2030, 2060, and 2090. The IIASA population scenario driving these estimates is the moderate B2 scenario.

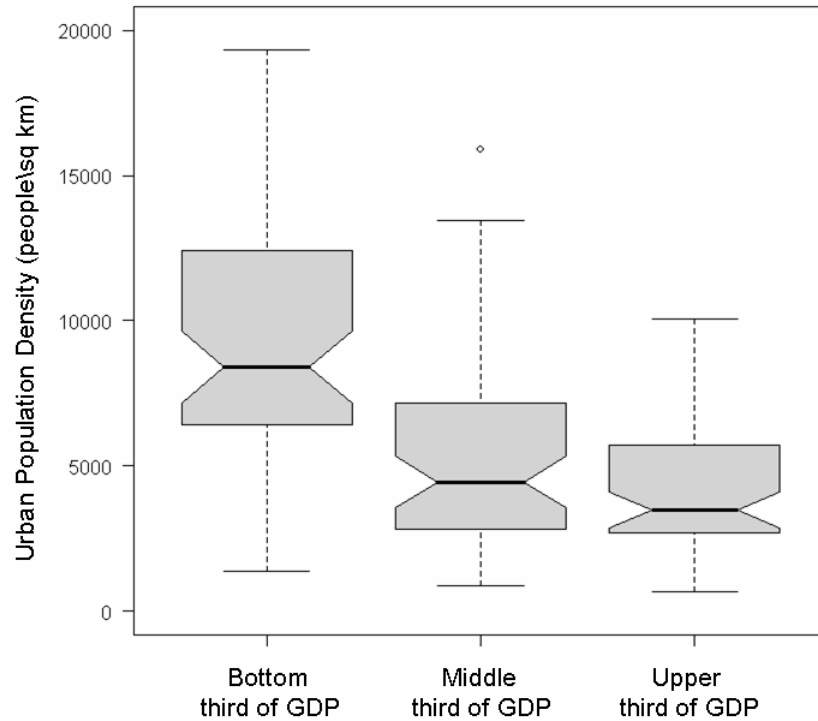


Figure 14. Relationship between urban population density and gross domestic product.

The GDP data comes from the IIASA SRES A2 model (Grubler et al. 2007) and is divided into three quantiles. The population densities are estimated using the MODIS 500 m urban map and the Grubler et al. urban population estimates for 2000. There are 185 countries included in this plot, with five high-density outliers not plotted.

REFERENCES

- Alberti, M., 2005. The effects of urban patterns on ecosystem function, *International Regional Science Review*, 28:2, 168-192.
- Allouche, O., A. Tsoar, R. Kadmon, 2006. Assessing the accuracy of species distribution models: prevalence, kappa and the true skill statistic (TSS), *Journal of Applied Ecology* 43:1223-1232.
- Angel, S., S.C. Sheppard, and D.L. Civco, 2005. *The Dynamics of Global Urban Expansion*. (Washington DC: The World Bank)
<http://www.williams.edu/Economics/UrbanGrowth/WorkingPapers.htm> (accessed April 15, 2007).
- Balk, D., T. Pullum, A. Storeygard, F. Greenwell, M. Neuman, 2004. A spatial analysis of childhood mortality in West Africa, *Population, Space and Place* 10: 175-216.
- Bartholome, E., and A.S. Belward, 2005. GLC2000: a new approach to global land cover mapping from Earth observation data, *International Journal of Remote Sensing* 26:1959-1977.
- Bengtsson, M., Y. Shen, T. Oki, 2007. A SRES-based gridded population dataset for 1990-2100, *Population and Environment* 28:113-131.
- Bhaduri, B., Bright, E., Coleman, P., and Dobson, J., 2002. LandScan: locating people is what matters, *Geoinformatics*, 5: 34-37.
- Bhaduri, B., Bright, E., Coleman, P., and Dobson, J., 2002. LandScan: locating people is what matters, *Geoinformatics*, 5: 34-37.

- Breiman, L, 2001. Random forests, *Machine Learning* 45:5-32.
- Brooks, T. *et al.*, 2004. Coverage provided by the global protected-area system: is it enough? *BioScience*, 54:12, 1081-1091.
- Bruner, A. *et al.*, 2004. Financial costs and shortfalls of managing and expanding protected-area systems in developing countries, *BioScience*, 54, 1119-1126.
- Burgess, N.D., A. Balmford, N.J. Cordeiro, J. Fjeldsa, W. Kuper, C. Rahbek, E.W. Sanderson, J.P.W. Scharlemann, J.H. Sommer, P.H. Williams, 2007. Correlations among species distributions, human density and human infrastructure across the high biodiversity tropical mountains of Africa, *Biological Conservation* 2:164-177.
- Calbo, J., Pan, W., Webster, M., Prinn, R. G., and McRae, G. J., 1998. Parameterization of urban sub-grid scale processes in global atmospheric chemistry models, *Journal of Geophysical Research*, 103: 3437-3467.
- Center for International Earth Science Information Network (CIESIN), 2004. Global Rural-Urban Mapping Project (GRUMP), Alpha Version: Urban Extents. <http://sedac.ciesin.columbia.edu/gpw> (Accessed April 15, 2007).
- Chape, S. *et al.*, 2005. Measuring the extent and effectiveness of protected areas as an indicator for meeting biodiversity targets, *Phil. Trans. R. Soc. B*, 360, 443-455.
- Cohen, J., 1960. A coefficient of agreement for nominal scales, educational and psychological measurement, 20:37-46.
- Congalton, R.G. and K. Green, 1999. Assessing the Accuracy of Remotely Sensed Data: Principals and Practices. New York: CRC Press.

- Danko, D.M., 1992. The Digital Chart of the World Project, *Photogrammetric Engineering and Remote Sensing*, 58:8, 1125-1128.
- Davies, G. et al., 2006. Human impacts and the global distribution of extinction risk, *Proc. R. Soc. B.*, 273, 2127-2133.
- Davies, R., C. Orme, V. Olson, G. Thomas, S. Ross, T. Ding, P. Rasmussen, A. Strattersfield, P. Bennett, T. Blackburn, I. Owens, K. Gaston, 2006. Human impacts and the global distribution of extinction risk, *Proceedings of the Royal Society B*, 273, 2127-2133.
- Dobson, J.E., E.A. Bright, P.R. Coleman, R.C. Durfee, and B.A. Worley, 2000. Landscan: A global population database for estimating populations at risk. *Photogrammetric Engineering and Remote Sensing*, 66:849-857.
- Elvidge, C., B.T. Tuttle, P.C. Sutton, K.E. Baugh, A.T. Howard, C. Milesi, B.L. Bhaduri, R. Nemani, 2007. Global Distribution and Density of Constructed Impervious Surfaces, *Sensors* 7:1962-1979.
- Folke, C., Jansson, A. Larsson, J., and Costanza, R., 1997. Ecosystem appropriation by cities, *Ambio*, 26: 167-172.
- Forbes, A.D., 1995. Classification algorithm evaluation: five performance measures based on confusion matrices, *Journal of Clinical Monitoring* 11:189-206.
- Gaffin, S.R., C. Rosenzweig, X. Xing, G. Yetman, 2004. Downscaling and geo-spatial gridding of socio-economic projections from the IPCC Special Report on Emissions Scenarios (SRES), *Global Environmental Change* 14: 105-123.

- Goldewijk, K., 2005. Three centuries of global population growth: A spatially referenced population density database for 1700 – 2000, *Population and Environment*, 26:5, 343-367.
- Grimm, N.B., S.H. Faeth, N.E. Golubiewski, C.L. Redman, J. Wu, X. Bai, J.M. Briggs, 2008. Global change and the ecology of cities, *Science* 319: 756-760.
- Greyner, R., C. Orme, S. Jackson, G. Thomas, R. Davies, T. Davies, K. Jones, V. Olson, R. Ridgely, P. Rasmussen, T. Ding, P. Bennett, T. Blackburn, K. Gaston, J. Gittleman, I. Owens, 2006. Global distribution and conservation of rare and threatened vertebrates, *Nature*, 444:2, 93-96.
- Grimm, N.B., S.H. Faeth, N.E. Golubiewski, C.L. Redman, J. Wu, X. Bai, J.M. Briggs, 2008. Global change and the ecology of cities, *Science* 319: 756-760.
- Grubler, A., B. O'Neill, K. Riahi, V. Chirkov, A. Goujon, P. Kolp, I. Prommer, S. Scherbov, E. Slentoe, 2007. Regional, national, and spatially explicit scenarios of demographic and economic change based on SRES, *Technological Forecasting and Social Change* 74: 980-1029.
- Herold, M., Goldstein, N. C., and Clarke, K.C., 2003. The spatiotemporal form of urban growth: measurement, analysis and modeling, *Remote Sensing of Environment*, 86: 286-302.
- Intergovernmental Panel on Climate Change, 2007. *Working Group II Report: Climate Change 2007, Impacts, Adaptation and Vulnerability – Summary for Policymakers*, IPCC Secretariat, Geneva, Switzerland.
- IUCN (1994). *Guidelines for Protected Areas Management Categories*. IUCN, Cambridge, UK and Gland, Switzerland. 261pp.

- Kendall, M., 1938. A New Measure of Rank Correlation, *Biometrika*, 30, 81-89.
- Lockwood, M., G.L. Worboys, A. Kothari, 2006. *Managing protected areas: a global guide*, Earthscan, London.
- Lutz, W. ed, 1996. *The future population of the world: what can we assume today?*
London: Earthscan.
- Lutz, W. W. Sanderson, and S. Scherbov, 2001. The end of world population growth,
Nature 412: 543-545.
- Montgomery, M., 2008. The urban transformation of the developing world, *Science* 319:
761-764.
- Montgomery, M., Stren, R., Cohen, B., and Reed, H. 2003. *Cities Transformed:
Demographic Change and Its Implications in the Developing World*, National
Academies Press, Washington, D.C.
- Morris, D.W., S.R. Kingston, 2002. Predicting future threats to biodiversity from habitat
selection by humans, *Evolutionary Research* 4:787-810.
- Myers, N., R. Mittermeier, C. Mittermeier, G. da Fonseca, J. Kent, 2000. Biodiversity
hotspots for conservation priorities, *Nature*, 403:24, 853-858.
- Nakicenovic, N., and R. Stuart, eds., 2000. *Special report on emissions scenarios: A
special report of working group III of the intergovernmental panel on climate change*.
Cambridge: Cambridge University Press.
- National Geophysical Data Center, 2007. Nighttime Lights data available at:
<http://www.ngdc.noaa.gov/dmsp/sensors/ols.html>.

- Olson, D.M., E. Dinerstein, E.D. Wikremanayake, N.D. Burgess, G.V.N. Powell, E.C. Underwood, J.A. D'Amico, I. Itoua, H.E. Strand, J.C. Morrison, C.J. Loucks, T.F. Allnutt, T.H. Ricketts, T. Kura, J.F. Lamoreux, W.W. Wittengel, P. Hedao, and K.R. Kassem, 2001. Terrestrial ecoregions of the world: a new map of life on Earth, *Bioscience* 51: 933-938.
- Pauchard, A, M. Aguayo, E Peria, and R. Urrutia, 2006. Multiple effects of urbanization on the biodiversity of developing countries: The case of a fast-growing metropolitan area (Concepcion, Chile), *Biological Conservation* 127: 272-281.
- Peters-Lidard, C. D., Kumar, S., Tian, Y., Eastman, J. L., and Houser, P., 2004. Global urban-scale land-atmosphere modeling with the land information system, *Symposium on Planning, Nowcasting, and Forecasting in the Urban Zone*, 84th American Meteorological Society Annual Meeting, 11-15 January 2004, Seattle, Washington, USA.
- Potere, D., A. Schneider, 2007. A critical look at representations of urban areas in global maps, *GeoJournal*, 69:55-80.
- Potere, D., in preparation. The geodetic accuracy of Google Earth's high resolution imagery archive.
- Rees, W.E., 1992. Ecological footprint and appropriated carrying capacity: what urban economics leaves out, *Environment and Urbanization*, 4: 121-130.
- Riahi, K., A. Grubler, N. Nakicenovic, 2007. Scenarios of long-term socio-economic and environmental development under climate stabilization, *Technological Forecasting and Social Change* 74: 887-935.

- Ricketts, T., M. Imhoff, 2003. Biodiversity, urban areas, and agriculture: locating priority ecoregions for conservation, *Conservation Ecology* 8:1-15.
- Rodrigues, A. *et al.*, 2004. Effectiveness of the global protected area network in representing species biodiversity, *Nature*, 428:8, 640-643.
- Sahr, K., D. White, A. Kimerling, 2003. Geodesic Discrete Global Grid Systems, *Cartography and Geographic Information Science*, 30:2, 121-134.
- Schneider, A., M.A. Friedl, D.K. Mciver, and C.E. Woodcock, 2003. Mapping urban areas by fusing multiple sources of coarse resolution remotely sensed data, *Photogrammetric Engineering and Remote Sensing* 69:1377-1386.
- Schneider, A., M.A. Friedl, and C.E. Woodcock, 2005. Mapping urban areas by fusing multiple sources of coarse resolution remotely sensed data: Global results, in *Proceedings of the 5th International Symposium of Remote Sensing of Urban Areas*, 14-16 March, Tempe, Arizona.
- Schneider, A., M. A. Friedl and D. Potere, in preparation. Monitoring the extent and intensity of urban areas globally using MODIS 500 m resolution satellite imagery.
- UN Population Division. 2005. *United Nations World Urbanization Prospects – The 2005 Revision*, <http://esa.un.org/unup> (accessed April 15, 2007).
- UN Statistics Division, 2008. <http://unstats.un.org/unsd/methods/m49/m49.htm>
- Unger, J., Sumeghy, Z., Bottyan, Z., and Musci, L., 2001. Land use and meteorological aspects of the urban heat island, *Meteorological Applications*, 8: 189-194.
- Van Vuuren, D.P., and B.C. O'Neill, 2006. The consistency of IPCC's SRES scenarios to recent literature and recent projections, *Climatic Change* 75: 9-46.

Van Vuuren, D.P., P.L. Lucas, H. Hilderink, 2007. Downscaling drivers of global environmental change: Enabling use of global SRES scenarios at the national and grid levels, *Global Environmental Change* 17:114-130.

World Database of Protected Areas, 2006. <http://www.unep-wcmc.org/wdpa> (Accessed 15 March 2008).

Zhang, X.Y., Friedl, M.A., Schaaf, C.B., Strahler, A.H., and Schneider, A., 2004. The footprint of urban climates on vegetation phenology. *Geophysical Research Letters*, 31:12, L12209.